Scaling of number, size, and metabolic rate of cells with body size in mammals

Van M. Savage*[†‡§¶], Andrew P. Allen[‖], James H. Brown[‡¶**], James F. Gillooly[††], Alexander B. Herman[‡§], William H. Woodruff[‡§], and Geoffrey B. West[‡§]

*Department of Systems Biology, Harvard Medical School, Boston, MA 02115; [†]Bauer Laboratory, Harvard University, 7 Divinity Avenue, Cambridge, MA 02138; [‡]Santa Fe Institute, 1399 Hyde Park Road, Santa Fe, NM 87501; [§]Los Alamos National Laboratory, Los Alamos, NM 87545; [‖]National Center for Ecological Analysis and Synthesis, Santa Barbara, CA 93101; **Department of Biology, University of New Mexico, Albuquerque, NM 87131; and [††]Department of Zoology, University of Florida, Gainesville, FL 32611

Contributed by James H. Brown, December 27, 2006 (sent for review November 15, 2006)

The size and metabolic rate of cells affect processes from the molecular to the organismal level. We present a quantitative, theoretical framework for studying relationships among cell volume, cellular metabolic rate, body size, and whole-organism metabolic rate that helps reveal the feedback between these levels of organization. We use this framework to show that average cell volume and average cellular metabolic rate cannot both remain constant with changes in body size because of the well known body-size dependence of whole-organism metabolic rate. Based on empirical data compiled for 18 cell types in mammals, we find that many cell types, including erythrocytes, hepatocytes, fibroblasts, and epithelial cells, follow a strategy in which cellular metabolic rate is body size dependent and cell volume is body size invariant. We suggest that this scaling holds for all quickly dividing cells, and conversely, that slowly dividing cells are expected to follow a strategy in which cell volume is body size dependent and cellular metabolic rate is roughly invariant with body size. Data for slowly dividing neurons and adipocytes show that cell volume does indeed scale with body size. From these results, we argue that the particular strategy followed depends on the structural and functional properties of the cell type. We also discuss consequences of these two strategies for cell number and capillary densities. Our results and conceptual framework emphasize fundamental constraints that link the structure and function of cells to that of whole organisms.

allometry | body mass | cell number | cell size | cell types

Many biological studies focus on how cellular properties affect the structure and function of the whole organism. Little attention, however, has been paid to the inverse problem: to what extent do whole-organism anatomy and physiology influence cell size and function? Both research directions are necessary to develop a comprehensive, integrated understanding of biological systems.

Of particular relevance is the scaling of cell size and cellular metabolic rate with body size. Both have important consequences for cellular and whole-body properties (1, 2), such as numbers of organelles, cells, and capillaries (1–5). There is little empirical consensus or theoretical understanding of how the numbers, sizes, and metabolic rates of cells change with body size. This lack of consensus is true despite numerous studies of cellular processes, including extensive work on cell size and genome length (1, 2, 5–20), across a broad spectrum of different-sized mammals and other organisms. Schmidt-Nielsen (21) concluded that "... large and small animals have cells that are roughly of the same size..." so that "... a large organism is not made up of larger cells, but of a larger number of cells of roughly the same size." This is the view predominantly expressed, or tacitly assumed, in much of the literature. However, exceptions to this pattern for certain cell types have been reported for almost a century. For example, empirical trends of increasing cell size with body size have been noted for both neurons and adipocytes, and theories specific to these tissues have been discussed (15–20). Indeed, D. Thompson (22) remarked that "..whereas such cells as continue to divide throughout life tend to uniformity of size in all mammals, those which do not do so, and in particular the ganglion cells, continue to grow and their size becomes, therefore, a function of the duration of life."

Theoretical Framework

In this article, we develop a theoretical framework for exploring the quantitative relationships between body size, cell size, and metabolic rate in mammals. We show how the scaling of whole-body metabolic rate, determined by the rate of oxygen consumption, plays a central role in determining the scaling of the size, number, and metabolic rate of different cell types. We begin by noting that whole-organism metabolic rate, B, scales approximately as $M^{3/4}$, where M is body mass (3, 21, 22–26). Mass-specific metabolic rate, B/M, therefore scales approximately as

$$\bar{B} \equiv \frac{B}{M} \propto M^{-1/4}. \quad [1]$$

In Fig. 1, we present empirical data for this relationship based on measurements of the oxygen consumption rates and the weights for 626 species of mammals that cover six orders of magnitude in body size.

Because the mass-specific metabolic rate represents the power consumed per gram, it can also be interpreted as the ratio of the average metabolic rate of a cell, B_c, to the average cell size, m_c: $B/M = B_c/m_c$. Thus, Eq. **1** can be expressed as

$$\bar{B} \equiv \frac{B_c}{m_c} \propto M^{-1/4}. \quad [2]$$

Interpreted in this way, Fig. 1 demonstrates that the ratio of average cellular metabolic rate to average cell size decreases with increasing body size according to Eq. **2**.

Eq. **2** explicitly links cellular properties with the whole organism. This link demands a specific tradeoff between average cellular metabolic rate and average cell size such that as whole-organism body mass, M, varies, B_c and m_c cannot both simultaneously remain constant. This tradeoff is surprising because, *a priori*, it might be expected that, as new species and lineages evolve, natural selection would conserve the characteristics of basic building blocks, such as cells, by keeping their fundamental properties, like size and metabolic rate, invariant. This apparent lack of parsimony in natural

Author contributions: V.M.S., J.H.B., W.H.W., and G.B.W. designed research; V.M.S., A.P.A., J.H.B., J.F.G., A.B.H., and G.B.W. performed research; V.M.S. and G.B.W. contributed new reagents/analytic tools; V.M.S., A.P.A., and J.F.G. analyzed data; and V.M.S., J.H.B., and G.B.W. wrote the paper.

The authors declare no conflict of interest.

Abbreviation: CI, confidence interval.

[¶]To whom correspondence may be addressed. E-mail: van_savage@hms.harvard.edu or jhbrown@umn.edu.

This article contains supporting information online at www.pnas.org/cgi/content/full/0611235104/DC1.

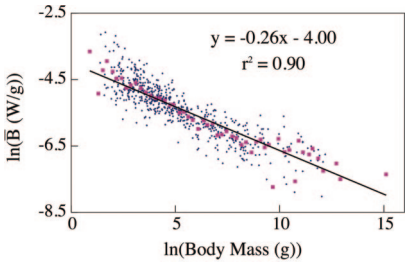

Fig. 1. Plot of the logarithm of the mass-specific metabolic rate, $\bar{B}$, versus the logarithm of body mass, M, for mammals. The data set is from Savage *et al.* (25), which contains a total of 626 species data points. The numerous small diamonds are the raw data. The data were binned to account for the bias toward species with small body masses, and the squares represent the average of the logarithms for every 0.1 log unit interval of mass (25). The regression line is fitted to the binned data (squares). Note that the mass-specific metabolic rate can be thought of as either the ratio of whole-organism metabolic rate to body mass, B/M (Eq. **1**) or the ratio of the average cellular metabolic rate to the average cell mass, B_c/m_c (Eq. **2**). It is clear that the mass-specific metabolic rate decreases with body mass with an exponent close to −1/4 [for the binned data the slope is −0.26 ($P < 0.0001$, $n = 52$, 95% C.I.: −0.29, −0.24)]. This relationship demands a tradeoff between cellular metabolic rate and cell mass as body mass varies.

selection revealed by Eq. **2** is a necessary consequence of the empirical fact that whole-body metabolic rate scales nonlinearly with body mass. This conclusion does not depend on the precise value of the allometric exponent nor on any theoretical model for understanding its origin.

Given that B_c and m_c cannot both remain constant simultaneously, two alternative selection strategies offer the next-simplest and most extreme possibilities: (*i*) average cell mass remains fixed (along with cell volume if cellular density is invariant), whereas average *in vivo* cellular metabolic rate varies

$$V_c \propto m_c \propto M^0 \quad B_c \propto M^{-1/4} \quad N_c \propto M \quad \text{and} \quad t_c \propto M^{1/4}, \qquad [3]$$

or, (*ii*) average cellular metabolic rate remains unchanged whereas average cell size varies

$$V_c \propto m_c \propto M^{1/4} \quad B_c \propto M^0 \quad N_c \propto M^{3/4} \quad \text{and} \quad t_c \propto M^0. \qquad [4]$$

Here, t_c represents cellular time scales that are closely tied to or determined by the metabolic processes and rates of the cell (27, 28). Because body mass is merely the product of cell number and average cell mass, it follows that strategy *i*, in which cell size remains fixed, requires that the number of cells, N_c, scales linearly with body mass. Additionally, because cellular metabolic rate scales as $B_c \propto M^{-1/4}$, time scales determined by cellular metabolism, which may include cell lifespan and cell-cycle time, must scale inversely as, $t_c \propto M^{1/4}$ (27, 28). Strategy *ii*, in which cell size varies, requires that the total number of cells increases nonlinearly with body mass and that associated time scales be invariant with respect to body mass. Intermediate strategies in which cellular metabolic rate and cell mass both vary with body mass, in a manner consistent with Eq. **2**, are also possible, but we note that strategies *i* and *ii* represent the simplest cases.

We include further detail about the cellular level by considering specific cell types and not just average cells. Because there are multiple cell types in the body, each with different characteristic sizes and metabolic rates [see supporting information (SI) *Materials and Methods*], whole-organism metabolic rate and body mass can be calculated by summing over all T cell types:

$$B = \sum_{k=0}^{T} N_{c,k} B_{c,k} \equiv N_c B_c \qquad [5]$$

and

$$M = \sum_{k=0}^{T} N_{c,k} m_{c,k} \equiv N_c m_c, \qquad [6]$$

where, for each cell type, k, the number of cells is $N_{c,k}$, the *in vivo* cellular metabolic rate is $B_{c,k}$, cell mass is $m_{c,k}$, and the total number of cells in the body is N_c, ($N_c = \Sigma_{k=0}^{T} N_{c,k}$). Thus, Eq. **2** could be reexpressed in terms of the ratios of the sums in Eqs. **5** and **6**, and average cellular metabolic rate and cell mass represent averages across all cell types.

Relationships between the scaling exponents for individual cell types and those for the whole organism are derived in *SI Materials and Methods*.

Results

We analyzed empirical data for the size and number of cells to discover whether they match our expectations for either of the two extreme strategies outlined above (Eqs. **3** and **4**), and thus, whether cell types can be classified according to these two strategies. We compiled data from the literature for mammalian species ranging in size from mice to elephants. We found data on cell size for 18 different cell types, and on cell number for 7 different cell types (see *SI Materials and Methods*). In this section and the associated figures, we use the notation V_c, N_c, m_c, and B_c for each cell type, not just averages across cell types, because this notation simplifies the presentation of the figures.

To test for the cell size relationships in Eqs. **3** and **4**, we plot the logarithm of cell volume, $\ln(V_c)$, against the logarithm of body mass, $\ln(M)$, for all cell types. We found that strategy *i* (Eq. **3**: invariant cell mass and scaling cellular metabolic rate) is consistent with the findings for the following 13 cell types: erythrocytes, fibroblasts, fibrocytes, goblet cells, hepatocytes, lung endothelial cells, lung interstitial cells, lung type I cells, lung type II cells, and cells from

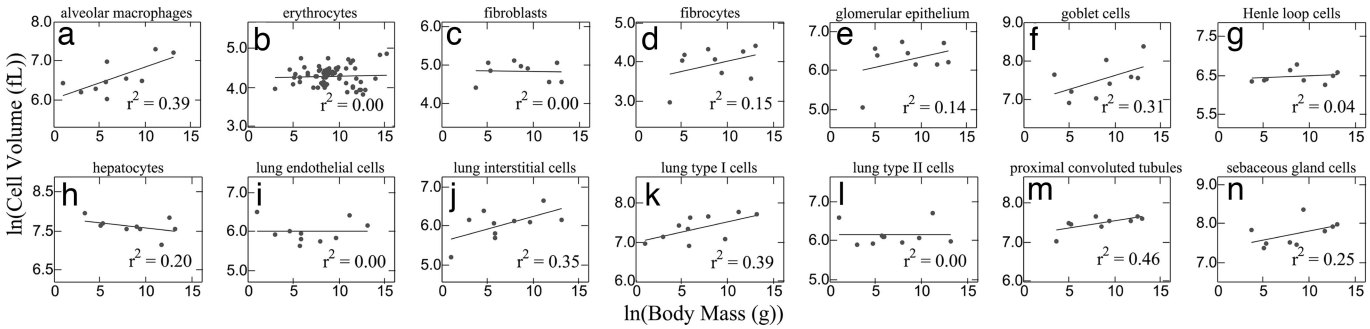

Fig. 2. Plots of the logarithm of cell volume versus the logarithm of body mass for 14 cell types that most closely follow strategy *i* (invariant cell mass and scaling cellular metabolic rate). Except for alveolar macrophages, the 95% CI of the slopes all include the value of 0 that is expected for strategy *i* (Table 1).

Table 1. Measurements and classifications for cell volume and cell number

Cell type	Strategy	Theoretical allometric exponent	Measured allometric exponent (slope *a*)	95% CI for *a*	*N*	y_{int}
Cell volume						
Alveolar macrophages	*i*	0	0.08	(0.01,0.14)	10	6.03
Erythrocytes	*i*	0*	0	(−0.02,0.03)	74	4.25
Fibroblasts	*i*	0*	0	(−0.07,0.06)	9	4.86
Fibrocytes	*i*	0*	0.05	(−0.06,0.16)	9	3.50
Glomerular epithelium	*i*	0*	0.05	(−0.07,0.18)	9	5.80
Goblet cells	*i*	0*	0.07	(−0.02,0.17)	9	6.90
Henle loop cells	*i*	0*	0.01	(−0.03,0.05)	9	6.39
Hepatocytes	*i*	0*	−0.03	(−0.08,0.02)	9	7.85
Lung endothelial cells	*i*	0*	0	(−0.06,0.06)	10	5.99
Lung interstitial cells	*i*	0*	0.06	(−0.01,0.13)	10	5.59
Lung type I cells	*i*	0*	0.05	(0.00,0.11)	10	7.00
Lung type II cells	*i*	0*	0	(−0.06,0.06)	10	6.14
Proximal convoluted tubules	*i*	0*	0.04	(0.00,0.07)	9	7.16
Sebaceous gland cells	*i*	0*	0.05	(−0.03,0.12)	9	7.34
Adipocytes (dorsal wall of abdomen)	*ii*	0.25	0.13	(0.02,0.23)	53	12.18
Adipocytes (skin)	*ii*	0.25*	0.17	(0.08,0.27)	9	8.88
Cerebellar granule neurons	*ii*	3/4 × 1/4 = 0.19*	0.14	(0.06,0.22)	9	3.56
Cerebellar Purkinje neurons	*ii*	3/4 × 1/4 = 0.19*	0.18	(0.14,0.23)	19	7.20
Number of cells						
Alveolar macrophages	*i*	1*	0.96	(0.86,1.06)	10	11.94
Lung endothelial cells	*i*	1*	1.00	(0.90,1.09)	10	14.32
Lung interstitial cells	*i*	1*	1.08	(0.97,1.19)	10	13.11
Lung type I cells	*i*	1*	0.95	(0.80,1.09)	10	13.12
Lung type II cells	*i*	1*	0.98	(0.92,1.14)	10	12.73
Adipocytes (dorsal wall of abdomen)	*ii*	0.75*	0.80	(0.73,0.88)	53	11.28
Superior cervical ganglion neurons	*ii*	0.75*	0.68	(0.51,0.85)	7	6.52

Each cell type (column 1) is classified as most closely following either strategy *i* or *ii* (column 2) as defined in the text. Strategy *i* corresponds to cellular metabolic rate scaling with body mass, M (in grams), and invariant cell volume, V_c (in fl), whereas strategy *ii* corresponds to invariant cellular metabolic rate and scaling of cell volume. According to the classification, the theoretical values for the allometric exponent of either cell volume or of cell number, N_c, are listed (column 3). (See *Discussion* and *SI Materials and Methods* for an explanation of these theoretical expectations.) For the cell volume data, allometric scaling exponents, a, were estimated by fitting linear regression models of the form $\log(V_c) = a\log(M) + y_{int}$. For the cell number data, exponents were estimated by fitting models of the form $\log(N_c) = a\log(M) + y_{int}$. The 95% CI of the fitted slope, the number of data points used for model fitting, and the fitted intercept are reported for each of the models depicted in Figs. 2–4 and SI Fig. 5. The data strongly support the values based on the strategy (*i* or *ii*). The average allometric exponent for cell volume for the cells following strategy *ii* is 0.16 (95% CI: 0.14,1.18) and for cells following strategy *i* is 0.03 (95% CI: −0.03,0.09).
*Predictions that lie within the 95% CI of measurements.

sebaceous glands, the glomerular epithelium, loop of Henle, and proximal convoluted tubules (Fig. 2). For all of these cell types, the slopes of the fitted lines yield exponents with 95% confidence intervals (CIs) that include the value of 0 (Table 1), consistent with strategy *i*. In addition, alveolar macrophages (Fig. 2) have an exponent with a 95% CI that nearly includes 0 and is far from the exponent of 1/4, making this cell type most consistent with strategy *i* but suggesting it is not accurately described by either of our two extreme strategies. For the four remaining cell types (granular and Purkinje neurons, and adipocytes from the dorsal wall of the abdomen, and s.c. deposits), we found that strategy *i* does not hold (Fig. 3) and that values for the allometric exponents are much closer to those for strategy *ii* (Eq. **4**: scaling cell mass and invariant cellular metabolic rate). Specifically, the fitted slopes (range: 0.13–0.18) all have 95% CIs >0, but that are somewhat lower than the value of 0.25 that would be consistent with strategy *ii* (Table 1). Possible reasons for these deviations are given in *Discussion*.

We also compiled data for cell number for seven cell types. Based on results in Figs. 2 and 3, five of these cell types (alveolar macrophages, lung endothelial cells, lung interstitial cells, lung type I cells, and lung type II cells) should follow strategy *i* more closely, and two of these cell types (adipocytes from the dorsal wall of the abdomen and superior cervical ganglion neurons) should follow strategy *ii* more closely. We plot cell number, $\ln(N_c)$, versus $\ln(M)$ to test this prediction, and indeed, this trend is what we find. Cell types that follow strategy *i* have allometric exponents with 95% CIs that include 1 for the scaling of cell number (Table 1 and SI Fig. 5), and cell types that follow strategy *ii* have exponents with 95% CIs that include 3/4 [0.80 for adipocytes (dorsal wall of abdomen) and 0.68 for superior cervical ganglion neurons (Table 1 and Fig. 4)].

To confirm that our two strategies require a tradeoff between cell volume and cellular metabolic rate for each cell type, we need data for cellular metabolic rates from a variety of cell types across a broad assortment of organisms. A direct test of the scaling of cellular metabolic rates predicted by Eqs. **3** and **4** requires *in vivo* measurements of oxygen consumption for specified cell types. Such data are exceedingly difficult to obtain but are becoming increasingly feasible with advances in imaging technology. Porter reviews evidence that mass-specific metabolic rate decreases with body size, approximately according to Eq. **1**, for specific cell types (29). Based on his and Brand's *in vitro* measurements, Porter determines that the mass-specific metabolic rate of hepatocytes scales as $M^{-0.18}$. Together with the above finding that hepatocyte cell mass is independent of body mass, this relationship suggests that their cellular metabolic rate decreases with body mass as $M^{-0.18}$. In addition, Davies (30) analyzed data obtained by Krebs (31) for *in vitro* measurements of oxygen consumption from tissue slices, which likely contain diverse cell types, and he calculated the exponents for the scaling of mass-specific metabolic rate with body mass to be −0.07 for brain, −0.07 for kidney, −0.17 for liver, −0.10 for lung,

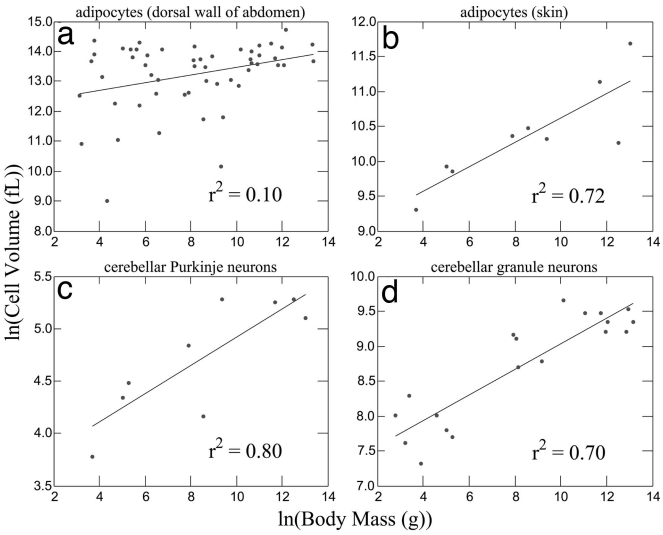

Fig. 3. Plots of the logarithm of cell volume versus the logarithm of body mass for four cell types that most closely follow strategy *ii* (scaling cell mass and invariant cellular metabolic rate). The 95% CIs of the slopes are all >0 and near the values expected for strategy *ii* (Table 1).

and −0.14 for spleen. Unfortunately, all of these data are based on only nine species of mammals and on *in vitro* measurements of tissue slices that have been isolated from their vascular supply, affecting the measured cellular metabolic rates. [Note that the *in vitro* data described in this paragraph were obtained from freshly harvested cells, not cells cultured for multiple generations. Thus, the scaling of these specific data are expected to approximate the scaling of *in vivo* cellular metabolic rate better than *in vitro* measures in general (2) but are still likely to be underestimates of the *in vivo* values (30)].

The total mitochondrial membrane surface area per volume of tissue has also been used as a proxy for mass-specific metabolic rate (32). These measures are much less direct than those previously mentioned because they are static, volumetric measures with no connection to oxygen or resource consumption and no units of time. Moreover, this proxy may be particularly poor for muscle tissue in which total mitochondria more closely reflects maximal, rather than basal or field, metabolic rate (33). The measured exponents for total mitochondrial membrane surface area per volume versus body mass are: −0.24 (95% CI: −0.33, −0.15) for liver, −0.22 (95% CI: −0.42, −0.02) for kidney, −0.11 (95% CI: −0.21, −0.01) for brain, −0.16 (95% CI: −0.28, −0.04) for heart, −0.07 (95% CI: −0.71, 0.55) for lung, and −0.23 (95% CI: −0.84, −0.38) for skeletal muscle (32). These values for the allometric exponents of mass-specific metabolic rates are higher (except for lung) than the ones

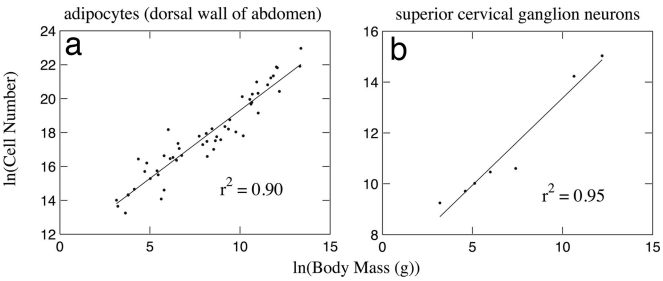

Fig. 4. Plots of the logarithm of cell number versus the logarithm of body mass for two cell types that most closely follow strategy *ii* (scaling cell mass and invariant cellular metabolic rate). The 95% CIs of the slopes all include the value of 0.75 corresponding to strategy *ii* (Table 1).

based on *in vitro* measures given above, and indeed, are generally closer to −1/4, consistent with the whole-organism scaling of mass-specific metabolic rate (Fig. 1). Note that if mass-specific metabolic rate and cell size both scale according to Eqs. **3** and **4**, consistent with data presented here, then the scaling of cellular metabolic rate must also follow these equations.

Discussion

Remarkably, almost all of the cell types for which we have data can be classified according to our two extreme strategies *i* and *ii*. Intermediate strategies, although certainly possible, require the coordinated evolution of multiple traits (e.g., cell size and metabolic rate) along with evolutionary changes in body size across phylogeny. This coordination could be achieved through gene networks, but we suggest that is more difficult than the evolutionary processes necessary to change cell size or cellular metabolic rate alone and, therefore, argue that intermediate strategies arise less often through the process of natural selection.

Nevertheless, there are reasons to believe that these two strategies do not fully capture the variation in cell mass with body mass. For example, the average of the exponents for cell types following strategy *i* is 0.03 (95% CI: −0.03,0.09), potentially indicating a slight positive trend for cell volume with body mass even for these cell types. In addition, alveolar macrophages and adipocytes from the dorsal wall of the abdomen have exponents with 95% CI that do not match strategy *i* or *ii*, as discussed below, and we only have a few cell types with which to test to strategy *ii* at all. Finally, for many cell types, data are only available for a limited number of species, resulting in large 95% CIs (Table 1). Given the amazing diversity of cell types in mammals and other organisms, only further experimental work will determine the true generality and applicability of our framework. Although the empirical data in the Results section provide support for our two strategies, more data for a broad assortment of organisms and cell types taken from carefully designed experiments, ideally performed *in vivo*, are required to fully resolve the range of strategies used by cells.

Alternative strategies for cell size scaling imply alternative investment strategies for apportioning metabolic energy to replacement versus maintenance of cells. Cell division and replacement are energy intensive and require a sizeable fraction of the cell's energy resources (see, e.g., chapter 10 in ref. 2). Lowering cellular metabolic rates, as in strategy *i*, could be accomplished by reducing cell division rates, and indeed, this reduction is consistent with the inverse scaling of cellular metabolic rate and associated time scales listed for strategy *i* (Eq. **3**). Moreover, cell maintenance requires substantial energy to maintain gradients at external cell membranes. Because cell walls define the surface area of the cell and surface area increases with cell size, larger cells would be expected to use more total energy than smaller cells, but because surface-area-to-volume ratios decline with cell size, larger cells are expected to use less energy per volume than smaller cells. This expected increase in total cellular energy with cell size, however, seemingly contradicts the prediction of strategy *ii* that cellular metabolic rate is constant as cell size increases. The use of extensive empirical data to determine the body mass dependence of cellular metabolic rates is thus crucial for testing the validity of our two strategies, especially strategy *ii*, and research to understand more deeply the scaling of cell wall gradients with cell size is also warranted.

A crucial remaining challenge is to predict which cell types follow which strategy. The strategy followed should depend on how cellular-level structure and function affect the time scales and the relative allocation to replacement versus maintenance discussed above. Most cell types, such as erythrocytes, leukocytes and other immune system cells, liver and pancreas cells, and most epithelial cells require frequent replacement to maintain function, turning over rapidly with many cell divisions to replace cells that differentiate and die during the lifespan of the organism. There are, however, a few cell types whose functionality suggests that it is

necessary for them to turn over slowly, if at all, during adult lifespan. For example, white adipocytes store energy, and their volume comprises the nucleus, cytoplasm, and primarily a triglyceride droplet. Although adipocyte cytoplasm is highly metabolically active under certain conditions, the triglyceride droplet is relatively inert and requires little maintenance, likely resulting in long lifespans for these cells. In contrast, neurons and muscle cells are among the most metabolically active cells in the body and require constant maintenance. However, because they would be difficult to replace without serious disruption to structural and functional integration, it is advantageous for them to have very long lifespans. Thus, different cell types in the body can be classified as either quickly or slowly dividing, and this classification is aligned with the structural and functional requirements of the cells.

The rate at which cells divide is closely tied to cellular metabolic rate and nutrient availability (see ref. 5 and chapters 7 and 16 in ref. 2), as evidenced by the elevated metabolic rate of quickly dividing cancer cells (34–36). For strategy *i*, where average cell size remains constant (Eq. **3**), we predict that cell turnover increases with decreasing body size as $M^{-1/4}$. Given that mass-specific metabolic rate shows this same scaling relationship ($\bar{B} \propto M^{-1/4}$), the increase in metabolic rate with decreasing body size provides fuel for higher cell turnover. Strategy *i* therefore allows for the possibility of short cell lifespans and rapid cell turnover. Quickly dividing cells, such as erythrocytes and hepatocytes, are therefore predicted to follow strategy *i*, Eq. **3**, so their size should be independent of body mass.

For strategy *ii*, however, turnover rates of cells are expected to be independent of body size (M^0) (Eq. **4**). Strategy *ii* therefore allows for the possibility that cell lifespan is of an indefinite length, limited only by the lifetime of the organism, but requires ongoing allocation of metabolic energy to maintenance. Slowly dividing cells, such as adipocytes and neurons, are therefore expected to most closely follow strategy *ii*, so their cell masses are predicted to scale roughly as $M^{1/4}$ with body size (Eq. **4**) and their numbers as $M^{3/4}$.

These predictions for which cell types follow which strategies are generally consistent with our findings in *Results*, but we now discuss possible explanations for the deviations observed for alveolar macrophages, adipocytes from the dorsal wall of the abdomen, and cerebellar granule and Purkinje neurons. The scaling exponent for the volume of alveolar macrophages is significantly higher than zero (Table 1), and this trend may be because alveolar macrophages phagocytose microbes, particles, and even erythrocytes. Depending upon what has been phagocytosed, the vacuoles in these macrophages will be of varying size, thus affecting the total volume of the cell. Consequently, the volume of alveolar macrophages likely depends more on the environment and specific substances that have been encountered than on the size of the organism in which it lives, likely placing it outside of our two extreme strategies.

The scaling exponent for adipocyte volumes from the dorsal wall of the abdomen is lower than would be predicted for strategy *ii* (Table 1), and the 95% CI is quite large considering the relative abundance of data. Compared with other cell types, adipocyte volumes are especially variable, even within a species, because of different functional roles for adipocytes in different parts of the body, e.g., metabolically active adipocytes like those from the dorsal wall of the abdomen versus structural adipocytes like those in the eye socket. In addition, environmental differences in resources and temperature can affect the size of adipocytes and relative proportion of depots. To deal with the first of these issues, we isolated our analyses to adipocytes from specific parts of the body: the dorsal wall of the abdomen and the skin. Ideally, we would also account for environmental differences in resources and temperature, but for the current data, we are ignorant of these conditions. (For cell number these effects may not be as important, as evidenced by the greatly reduced variation for these data seen in Fig. 4.) It is very likely that environmental effects cause the large uncertainty in the scaling exponent for adipocyte volume. For these same reasons, it is difficult to determine the allometric scaling relationship for the total tissue volume of adipocytes. If this scaling relationship is nonlinear with body mass, additional effects may change the expected scaling for cell volume, as now explained for the brain and certain neurons.

The fact that the cell sizes of two types of neurons, granule and Purkinje, have scaling exponents substantially $<1/4$ may have a simple explanation. Some organs, e.g., the brain, receive their blood supply from a nearly autonomous part of the cardiovascular system. Consequently, following the theory of West *et al.* (26), organ metabolic rates are expected to scale as $B_j \propto M_j^{3/4}$, where M_j is the mass of the organ. Given that the mass of most organs scales nearly linearly with body mass (i.e., $M_j \propto M^{p_j}$, $p_j = 1$ in *SI Materials and Methods*) (21, 23), their metabolic rates should scale with body size in the same way as whole-organism metabolic rate ($B_j \propto M_j^{3/4} \propto M^{3/4} \propto B$). The brain, however, is a major exception. Its mass scales as $M_{\text{brain}} \propto M^{3/4}$ ($p_{\text{brain}} = 3/4$ in *SI Materials and Methods*) (23, 37, 38). This relationship suggests that brain neuron cell size (as opposed to neurons in other parts of the body such as superior cervical ganglion neurons) should scale as $M_{\text{brain}}^{1/4} \propto (M^{3/4})^{1/4} = M^{0.1875}$, and that brain neuron number should scale as $M_{\text{brain}}^{3/4} \propto (M^{3/4})^{3/4} = M^{0.5625}$. The measured exponents for the cell volumes of cerebellar Purkinje and granule neurons in Table 1 are consistent with these predicted exponents.

This prediction requires some minor corrections because the proportion of brain mass composed of neurons, as reflected in the relative quantities of gray and white matter, scales weakly with brain mass (39). Additional corrections may arise because the fraction of brain mass composed of different parts of the brain (e.g., telencephalon and medulla) can also scale with brain mass (40), and these different brain parts potentially correspond to different types of neurons. More detailed considerations of the constraints that neuronal function (e.g., conduction velocity) places on neuronal size and structure are analyzed by Wang and colleagues (41, 42), and this rich complexity of neuronal architecture may lead to further refinement of our arguments. Finally, it is noteworthy that the hippocampus and olfactory bulb are the two brain areas in which neurons are replaced regularly on a large scale. Therefore, we predict that the size of adult-generated neuron types from these brain regions should be independent of body size, in distinct contrast to the scaling behavior of other neurons.

The alternative strategies given by Eqs. **3** and **4** can be further interpreted in terms of the theoretical framework proposed by West *et al.* (26) for understanding the origin of the 3/4 exponent in Eq. **1**. This theory is based on generic properties of optimized, space-filling vascular networks that deliver vital resources, such as oxygen, to cells (26). An important assumption of the theory, motivated by natural selection, is that the physical properties of the terminal units of these networks are invariant with respect to body mass. In the circulatory system, not only is the size of capillaries assumed to be invariant, but so too is their blood flow rate, which ultimately determines the rate of resource delivery and therefore, the metabolic rate. This constancy of structural and functional properties of capillaries stands in distinct contrast to the inability of cells to maintain simultaneously the constancy of both size and metabolic rate. Indeed, the invariance of capillary parameters dictates that not all cell parameters, e.g., cell size and metabolic rate, can be invariant with respect to body mass. Empirical data for mammals support the assumption of invariance of capillary size and flow rate and of the size of erythrocytes and leukocytes (21, 23).

Independent of whether cell size remains constant or scales with body size, West *et al.* (26) predict that capillary density scales as $M^{-1/4}$. However, the alternative strategies described by Eqs. **3** and **4** lead to different predictions for the number of capillaries relative to the number of cells. For cell types that are invariant in size (strategy *i*), the number of capillaries per cell is predicted to decrease with increasing body size as $M^{-1/4}$, the original prediction of West *et al.* (26). For cell types such as nerve, muscle, and fat, where cell size increases with body size as approximately $M^{1/4}$

(strategy *ii*), the number of capillaries per cell is predicted to be approximately invariant. This prediction is consistent with cellular metabolic rate being independent of body size for these cell types because the metabolic power supplied by an individual capillary is invariant and the number of cells receiving that power is invariant. The exact relationships may be complicated because of specific geometrical constraints. For example, a substantial fraction of the volume of most neurons is composed of axons and dendrites, which would be expected to vary in length with body size. Cardiac and skeletal muscle cells similarly tend to increase much more in length than in diameter with increasing body size.

It would be instructive to understand better the architecture of capillary supply to different tissues, as well as the sizes, division rates, and lifespans of different cell types *in vivo* and *in vitro*, and the densities and turnover rates of cellular components such as mitochondria and enzymes. Additionally, it would be of great interest to determine empirically and to understand theoretically the scaling of the sizes and metabolic rates of mammalian stem cells. Because stem cells divide frequently, the framework developed here would naively predict that sizes of stem cells should remain invariant and that their *in situ* metabolic rates should scale as $M^{-1/4}$ across species. These same predictions should also apply to brown adipocytes, which can be highly metabolically active and divide rapidly, providing a strong contrast with the white adipocytes discussed in this article.

The critical point is that the theory dictates how generic properties of the vascular network constrain resource supply to cells. The structure and function of the vascular system and the associated $M^{3/4}$ scaling of whole-organism metabolic rate implies that it is impossible for all of the fundamental properties of cells to remain invariant as body size changes during both ontogeny and phylogeny. Depending on the structural and functional properties of cell types, either cell size, cellular metabolic rate, or possibly both, must change as body size varies through ontogeny and phylogeny.

Methods

Data used in Figs. 2–4 are given in SI Tables 2–4. We required that at least six data points be available for a cell type to be included in our analyses. Data were taken from the references that are listed therein. The methods for obtaining and measuring each cell type are detailed in these original references. When different studies measured values for the same cell type, we combined the data into a single dataset. When multiple values of a given cell type were reported for a given species, the geometric mean of values was used for analysis. We did not, however, average values for Fisher 344 and Sprague–Dawley rats because these rats may be considerably different metabolically and because the original source did not average these values. We also excluded data for cerebellar Purkinje neurons from Friede (15), which largely disagreed with more recent values from (12, 13), because, as stated there, these measures were meant to facilitate interspecies comparisons but not to establish absolute values for cell volume. Redoing the statistics and figures with the average for rats discussed above or the data from Friede has almost no influence on the exact numbers in Table 1 and does not affect any of our conclusions.

For adipocytes, data from 15 depots throughout the body were provided by C. M. Pond (The Open University, Milton Keynes, U.K.). Because of differing resource availability for the sampled mammals, exponents for cell size were variable across depots. In this article, we use only adipocytes from the dorsal wall of the abdomen (specifically from a depot sometimes called the retroperitoneal that includes perirenal adipose tissue and extends along the inner wall of the abdomen into the pelvis) because they are representative of general storage adipose (C. M. Pond, personal communication).

Allometric exponents were determined by using ordinary least squares (OLS) regression on ln-ln plots of the data. See Methods in ref. 38 for more information. CIs and *P* values were computed by using Mathematica (Wolfram Research, Inc., Champaign, IL).

We thank C. M. Pond and C. A. Mattacks (The Open University, Milton Keynes, U.K.) for providing us with data for cell size and cell number for adipocytes. C. M. Pond was extremely helpful in converting the data into a format we could use, in advising us as to which adipose depots were the best to use for our analyses, and in providing clarifying comments about the paper. We thank Timothy J. Mitchison for insightful comments on the manuscript and gratefully acknowledge Michelle Girvan for many helpful ideas. We also thank the reviewers, Samuel Wang and David Atkinson, for their thoughtful comments. V.M.S. also acknowledges support from National Institutes of Health Grant P50 GM68763, through the Bauer Laboratory, and Walter Fontana's laboratory at Harvard Medical School. A.P.A., J.H.B., J.F.G., and G.B.W. were supported in part by National Science Foundation Grant DEB-0083422. A.P.A. was supported as a Postdoctoral Associate at the National Center for Ecological Analysis and Synthesis, a center funded by National Science Foundation Grant DEB-0072909, and the University of California, Santa Barbara. J.H.B. and G.B.W. were also supported in part by a Packard Interdisciplinary Science Grant, and J.F.G. was supported in part by the Department of Zoology at the University of Florida. W.H.W. is grateful for support by National Institutes of Health Grant DK36263.

1. Atkinson D, Morley SA, Hughes RN (2006) *Evol Dev* 8:202–214.
2. Hall MN, Raff M, Thomas G, eds (2004) *Cell Growth: Control of Cell Size* (Cold Spring Harbor Laboratory Press, Cold Spring Harbor, NY).
3. West GB, Woodruff WH, Brown JH (2002) *Proc Natl Acad Sci USA* 99:2473–2478.
4. Gillooly JF, Allen AP, Brown JH, Elser JJ, Martinez del Rio C, Savage VM, West GB, Woodruff WH, Woods HA (2005) *Proc Natl Acad Sci USA* 102:11923–11927.
5. Jorgensen P, Tyers M (2004) *Curr Biol* 14:R1014–R1027.
6. Murray A, Hunt T (1993) *The Cell Cycle: An Introduction* (Oxford Univ Press, New York).
7. Partridge L, Barrie B, Fowler K, French V (1994) *Evolution (Lawrence, Kans.)* 48:1269–1276.
8. Cavalier-Smith T, ed (1985) *The Evolution of Genome Size* (John Wiley, Chichester, UK)
9. Gregory TR (2001) *Biol Rev* 76:65–101.
10. Lynch M, Conery JS (2003) *Science* 302:1401–1404.
11. Kozlowski J, Konarzewski M, Gawelczyk AT (2003) *Proc Natl Acad Sci USA* 100:14080–14085.
12. Morgado E, Ocqueteau C, Cury M, Becker L, Gonzalez U, Muxica L, Gunther B (1990) *Arch Biol Med Exp* 23:21–27.
13. Maldonado R, San Jose H, Martinoya C, Gunther B (1974) *Acta Physiol Latinoamerica* 24:328–335.
14. Stone KC, Mercer RR, Gehr P, Stocksill B, Crapo JD (1992) *Am J Respir Cell Mol Biol* 6:235–243.
15. Friede RL (1963) *Proc Natl Acad Sci USA* 49:187–193.
16. Mayhew TM (1991) *J Comp Neurol* 308:162–168.
17. Purves D, Rubin E, Snider WD, Lichtman J (1986) *J Neurosci* 6:158–163.
18. Pond CM, Mattacks CA (1985) *J Morphol* 185:183–193.
19. Pond CM, Mattacks CA (1986) *J Zool (London)* 209:35–42.
20. Bekkers JM, Stevens CF (1990) *Prog Brain Res* 83:37–45.
21. Schmidt-Nielsen K (1984) *Scaling: Why Is Animal Size So Important?* (Cambridge Univ Press, Cambridge, UK).
22. Thompson DAW (1942) *On Growth and Form* (Cambridge Univ Press, Cambridge, UK).
23. Peters RH (1983) *The Ecological Implications of Body Size* (Cambridge Univ Press, Cambridge, UK).
24. Calder WA (1984) *Size, Function, and Life History* (Harvard Univ Press, Cambridge, MA).
25. Savage VM, Gillooly JF, Woodruff WH, West GB, Allen AP, Enquist BJ, Brown JH (2004) *Funct Ecol* 18:257–282.
26. West GB, Brown JH, Enquist BJ (1997) *Science* 276:122–126.
27. Gillooly JF, Charnov EL, West GB, Savage VM, Brown JH (2002) *Nature* 417:70–73.
28. Lindstedt L, Schaeffer PJ (2002) *Lab Anim* 36(1):1–19.
29. Porter RK (2001) *Cell Mol Life Sci* 58:815–822.
30. Davies M (1961) *J Cell Comp Physiol* 57:135–147.
31. Krebs HA (1950) *Biochem Biophys Acta* 4:249–269.
32. Else PL, Hulbert AJ (1985) *Am J Physiol Regul Integr Comp Physiol* 248:R415–R421.
33. Weibel ER, Bacigalupe LD, Schmitt B, Hoppeler H (2004) *Respir Physiol Neurobiol* 140:115–132.
34. Loo WTY, Fong JHM, Cheung MNB, Chow LWC (2005) *Biomed Pharmacol* 59:S337–S339.
35. Cao Y, Sundgren PC, Tsien CI, Chenevert TT, Junck L (2006) *J Clin Oncol* 24:1228–1235.
36. Shields AF (2006) *Mol Imaging Biol* 8:141–150.
37. Pagel MD, Harvey PH (1988) *Am Nat* 132:344–359.
38. Savage VM, West GB (2007) *Proc Natl Acad Sci USA* 104:1051–1056.
39. Zhang K, Sejnowski TJ (2000) *Proc Natl Acad Sci USA* 97:5621–5626.
40. Clark DA, Mitra PP, Wang, SS-H (2001) *Nature* 411:189–193.
41. Harrison KH, Hof PR, Wang SS-H (2002) *J Neurocytol* 30:289–298.
42. Wittenberg GM, Wang SS-H, in *Dendrites*, eds Häusser M, Spruston N, Stuart G (Oxford Univ Press, Oxford), 2nd Ed, in press.